

# Nonlinear Image Restoration in Confocal Microscopy: Stability under Noise \*

J.B.T.M. Roerdink

*Institute for Mathematics and Computing Science*  
*University of Groningen, P.O. Box 800, 9700 AV Groningen, The Netherlands*  
*Tel. +31-50-633931; Fax +31-50-633800; Email roe@cs.rug.nl*

**ABSTRACT** — In this paper we study the noise stability of iterative algorithms developed in [1,2] for attenuation correction in Fluorescence Confocal Microscopy using FFT methods. In each iteration the convolution of the previous estimate is computed. It turns out that the estimators are robust to noise perturbation.

## 1 Introduction

One of the problems in 3D imaging by a CSLM (confocal scanning laser microscope) in the so-called (epi)fluorescence mode is the darkening of the deeper layers due to scattering and absorption of excitation and fluorescence light. Recently we developed a new restoration method, called the ‘FFT-method’, to correct for this attenuation effect [2]. Essential in this method is the computation of a correction factor in the form of a 3D convolution of the measured signal, which can be efficiently computed by the use of the Fast Fourier Transform (FFT). The complexity of computation of this method is to  $\mathcal{O}(N_z \log N_z)$ , where  $N_z$  is the number of vertical layers. In contrast, the iterative ‘layer stripping’ method (with condensation) developed in [3] has complexity  $\mathcal{O}(N_z^2)$ , with only slightly better restoration quality.

In an extension of this method we showed that the accuracy of the FFT-method can be improved by first order moment and cumulant estimators leading to a nonlinear integral equation for the unknown fluorescent density, which is solved by an iterative method [1].

The purpose of the present paper is to study the stability of our restoration method under noise perturbation. In particular we perturb the (simulated) data by Gaussian or Poisson noise and compare the behavior of the FFT method with that of the layer method.

The organization of this paper is as follows. In Section 2 we review the CSLM imaging process and discuss the reformulation of the CSLM transform as a statistical averaging problem with corresponding first order moment and cumulant estimators. We give an iterative algorithm to solve the resulting nonlinear integral equations for the object density. The stability under noise is studied in Section 3. Section 4 contains a summary and conclusions.

## 2 The CSLM transform

The CSLM imaging process leads to the following nonlinear integral transform (‘CSLM-transform’):

$$f(\mathbf{r}) = \rho(\mathbf{r}) \times \gamma_f(\mathbf{r}) \gamma_b(\mathbf{r}), \quad (1)$$

where  $f(\mathbf{r})$  is the measured fluorescent intensity at the point  $\mathbf{r}$ ,

$$\begin{aligned} \gamma_f(\mathbf{r}) : &= C_f \int_0^\omega d\theta \int_0^{2\pi} d\phi \sin \theta \cos \theta \\ &\times \exp \left[ -\varepsilon \int_0^z \frac{dz'}{\cos \theta} \rho(\hat{\mathbf{r}}) \right] \end{aligned} \quad (2)$$

is the forward attenuation factor, and

$$\begin{aligned} \gamma_b(\mathbf{r}) : &= C_b \int_0^\omega d\theta \int_0^{2\pi} d\phi \sin \theta \\ &\times \exp \left[ -\varepsilon \int_0^z \frac{dz'}{\cos \theta} \rho(\hat{\mathbf{r}}) \right] \end{aligned} \quad (3)$$

is the backward attenuation factor. In these equations  $\varepsilon$  is the attenuation constant and  $C_f$  and  $C_b$  are normalization constants:

$$C_f := \frac{1}{\pi \sin^2 \omega}, \quad C_b := \frac{1}{2\pi(1 - \cos \omega)}.$$

Here  $\theta$  and  $\phi$  are the polar angles of a light ray with respect to the  $z$ -axis (chosen along the optical axis), cf. Fig. 1, while  $\hat{\mathbf{r}}$  is the vector

$$\hat{\mathbf{r}} = \begin{pmatrix} x + (z - z') \tan \theta \cos \phi \\ y + (z - z') \tan \theta \sin \phi \\ z' \end{pmatrix}. \quad (4)$$

\*In: Proc. IEEE Workshop on Nonlinear Signal and Image processing, June 20-22, Neos Marmaras, Halkidiki, Greece, I. Pitas (ed.), 1995, pp. 750-753. Postscript version obtainable at <http://www.cs.rug.nl/roe/>

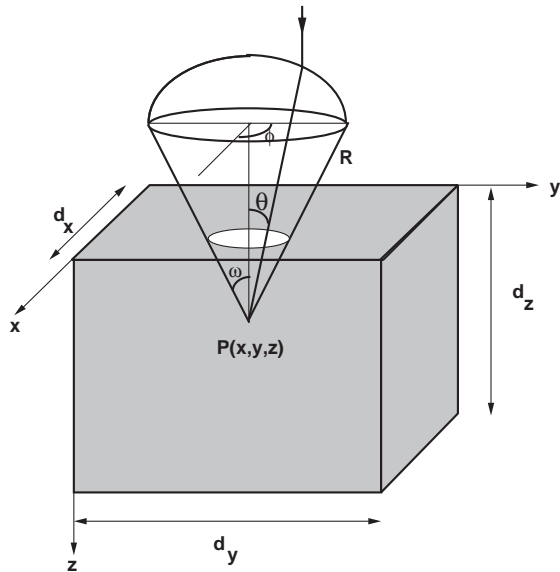


Figure 1: *CSLM geometry*.  $R$ : radius of spherical bundle;  $\omega$ : semi-aperture angle;  $(\theta, \phi)$ : polar angles of light ray;  $d_z$ : depth of the sample.

## 2.1 Inversion of the CSLM transform

Assuming weak attenuation one may carry out a perturbation expansion in the parameter  $\varepsilon$ , and derive the following approximation  $\tilde{\rho}(\mathbf{r})$  for the fluorescent density [2]

$$\tilde{\rho}(\mathbf{r}) = f(\mathbf{r}) \{1 + \varepsilon c(\mathbf{r})\}, \quad (5)$$

where  $c(\mathbf{r})$  is the convolution integral

$$c(\mathbf{r}) = \int_{-\infty}^{\infty} \int_{-\infty}^{\infty} \int_{-\infty}^{\infty} d\mathbf{r}' \kappa(\mathbf{r}') f(\mathbf{r} - \mathbf{r}') \quad (6)$$

with  $\kappa(\mathbf{r})$  the space-invariant kernel given by

$$\kappa(x, y, z) = C_f \frac{z}{(x^2 + y^2 + z^2)^{3/2}} + C_b \frac{1}{x^2 + y^2 + z^2}$$

for  $0 \leq z \leq d_z$ ,  $x^2 + y^2 \leq (z \tan \omega)^2$  and  $\kappa(x, y, z) = 0$  elsewhere.

## 2.2 Iterative algorithms

By applying moment and cumulant expansions of characteristic functions and after discretization, one can derive a finite system of nonlinear equations of the form

$$R_{ijk} = F_{ijk} G((K * R)_{ijk}), \quad (7)$$

where  $G(x) = \exp(\varepsilon x)$  for the cumulant approximation and  $G(x) = (1 - \varepsilon x)^{-1}$  for the moment

approximation, respectively, with  $K * R$  the discrete convolution of the 3D arrays  $K$  and  $R$  [1]. Here  $R_{ijk}$ ,  $F_{ijk}$  and  $K_{ijk}$  are the discrete counterparts of the estimated fluorescent density  $\tilde{\rho}(\mathbf{r})$ , the measured image density  $f(\mathbf{r})$ , and the convolution kernel  $\kappa(\mathbf{r})$ .

The solution of (7) leads to the following iterative algorithm:

1. Read the data  $F_{ijk}$ .
2. Determine the appropriate value of  $\varepsilon$ .
3. Iteratively compute ( $n = 1, 2, 3, \dots$ )

$$R_{ijk}^{(n)} = F_{ijk} G((K * R^{(n-1)})_{ijk}), \quad (8)$$

where  $R_{ijk}^{(0)} = F_{ijk}$ , and  $G(x) = (1 - \varepsilon x)^{-1}$  or  $G(x) = \exp(\varepsilon x)$  for the moment and cumulant estimator, respectively.

In each iteration the convolution of the previous estimate is computed by means of the FFT (using the same kernel  $K$  as defined above). The first iterate of (8) with  $G(x) = 1 + \varepsilon x$  coincides with the discrete analogon of (5) and is the approximation used in [2].

Input parameters of the algorithm are the dimensions  $N_x, N_y, N_z$  of the data array, the scanning steps  $\delta_x, \delta_y, \delta_z$ , the semi-aperture angle  $\omega$  and the attenuation constant  $\varepsilon$ . For the determination of the correct value of  $\varepsilon$  one may resort to a calibration experiment in which a homogeneous test sample is used [3]. In this paper we will consider test densities for which the value of  $\varepsilon$  is known.

## 3 Stability under noise

In this section we will consider the situation where the data are perturbed by additive or multiplicative noise. Error estimates will be derived which show that the behavior of the FFT method is stable under such perturbations. We will carry out the analysis for the algorithm with one iteration step only. The extension to two or more iterations is straightforward. However, more than two iterations will not be used in practice, because the computation time would increase to much. Moreover, the noise stability will become worse when many iterations are used. For the same reason one may expect sensitivity to noise of the iterative layer method of Visser et al. [3], which uses  $N_z$  iterations ( $N_z$  being the number of vertical layers).

### 3.1 Additive noise

Assume that the data  $f(\mathbf{r})$  are perturbed by additive noise  $n(\mathbf{r})$ . Then instead of (1) we have:

$$f(\mathbf{r}) = \rho(\mathbf{r}) \times \gamma_f(\mathbf{r})\gamma_b(\mathbf{r}) + \alpha n(\mathbf{r}). \quad (9)$$

We assume that the magnitude of the noise is bounded by the constant  $\alpha$ , so that  $|n(\mathbf{r})| \leq 1$ . As a measure of the restoration quality we use the difference between original density  $\rho(\mathbf{r})$  and restored density  $\tilde{\rho}(\mathbf{r})$ :

$$E(\mathbf{r}) = |\rho(\mathbf{r}) - \tilde{\rho}(\mathbf{r})|.$$

The restored density satisfies the equation

$$\tilde{\rho}(\mathbf{r}) = f(\mathbf{r}) \left\{ 1 + M[(\kappa * \tilde{\rho})(\mathbf{r})] \right\}$$

When only one iteration is used this becomes

$$\tilde{\rho}(\mathbf{r}) = f(\mathbf{r}) \left\{ 1 + M[(\kappa * f)(\mathbf{r})] \right\} \quad (10)$$

For the function  $M[x]$  we consider the following forms:

$$\begin{aligned} M[x] &= \exp(\varepsilon x) - 1 \\ M[x] &= \varepsilon x (1 - \varepsilon x)^{-1} \\ M[x] &= \varepsilon x \end{aligned}$$

The first of these applies to the cumulant approximation, the second to the moment approximation. The third form is included for comparison with the original approximation (5) as derived in [2]. Note that in all cases  $M[x]$  is a monotonically increasing function.

The key estimate we need is the following (cf. [2]). For any continuous function  $g(\mathbf{r})$ ,

$$|\kappa * g(\mathbf{r})| \leq \frac{2zg_{\max}}{\cos \omega}, \quad (11)$$

where  $g_{\max}$  is the maximum value of the function  $g(\mathbf{r})$ . Let  $\rho_{\max}$  be the maximum value of the original density  $\rho$ . Then, using methods similar to those used in the Appendix of [2], one can derive

$$E(\mathbf{r}) \leq \frac{2\rho_{\max}^2 \varepsilon z}{\cos \omega} + (\rho_{\max} + \alpha) M \left[ \frac{2z(\rho_{\max} + \alpha)}{\cos \omega} \right] + \alpha.$$

For example, when  $M[x] = \varepsilon x$  this formula reduces to

$$E(\mathbf{r}) \leq \frac{2\varepsilon z}{\cos \omega} \left( \rho_{\max}^2 + (\rho_{\max} + \alpha)^2 \right) + \alpha.$$

When there is no noise ( $\alpha = 0$ ) this formula agrees with that in the Appendix of [2].

### 3.2 Multiplicative noise

Let the data  $f(\mathbf{r})$  be perturbed by multiplicative noise, i.e.,

$$f(\mathbf{r}) = (1 + \alpha n(\mathbf{r})) \rho(\mathbf{r}) \times \gamma_f(\mathbf{r})\gamma_b(\mathbf{r}). \quad (12)$$

An example is impulsive noise, where  $n(\mathbf{r}) = 1$  with probability  $p$  and  $n(\mathbf{r}) = 0$  with probability  $1 - p$ , with  $0 \leq p \leq 1$ . In this case the estimate for the approximation (10) is

$$E(\mathbf{r}) \leq \rho_{\max} \left\{ \alpha + (1 + \alpha) \left( \beta \varepsilon + M[\beta(1 + \alpha)] \right) \right\}$$

with  $\beta = (2\rho_{\max}z)/\cos \omega$ . When  $M[x] = \varepsilon x$  this formula reduces to

$$E(\mathbf{r}) \leq \rho_{\max} \left\{ \alpha + (1 + \alpha)(2 + \alpha) \frac{2\rho_{\max} \varepsilon z}{\cos \omega} \right\}.$$

It is clear from the formulas in this and the previous subsection that the behavior of the algorithm under the influence of noise is essentially the same as when the noise is absent.

### 3.3 Restoration of noisy test images

We show restorations for an image consisting of circles ('circle image') perturbed by Gaussian noise, and a sinusoidally varying image ('trig image') perturbed by Poisson noise. One level of the original is shown in Fig. 2. All 8 depth layers of the original image are identical. Signal data  $F_{ijk}$  were generated by numerically computing the integrals in (2)–(3) for a number of equidistant 3D positions. The parameters were chosen as follows:  $d_x = d_y = 1.0$ ,  $d_z = 0.1$ ,  $N_x = N_y = 128$ ,  $N_z = 8$ ,  $\omega = 1.04719$ .

The noisy attenuated images were restored by the FFT method (moment estimator, 2 iterations), as well as the layer method of [3]. Results are shown in Fig. 3 and Fig. 4. The first row shows the noisy attenuated test images; the second row the restoration by the layer stripping method; the third row the restoration by the FFT method. In each row, the first, fourth and seventh layer is displayed from left to right. Computations were performed on a HP 9000/735 workstation (130 MIPS), taking about 15 seconds per iteration step.

We conclude that the FFT method is stable under noise perturbation. The layer stripping method has greater noise reduction effect, due to the implicit averaging procedure. However, we observe the occurrence of an 'inverted' noise (the black dots in the white regions), suggesting a certain instability of the algorithm. This may be due

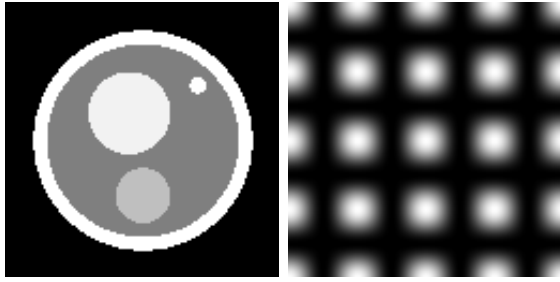


Figure 2: *One layer of original circle (left) and trig (right) images.*

to the fact that in layer stripping methods errors made in the first layers will propagate to deeper layers.

#### 4 Conclusions

In this paper we study the noise stability of iterative algorithms developed in [1,2] for attenuation correction in Fluorescence Confocal Microscopy using FFT methods. By a statistical reformulation of the problem it is possible to derive first order moment and cumulant estimators leading to a nonlinear integral equation for the unknown fluorescent density, which can be solved by an iterative method. The estimators are robust to noise perturbation, this in contrast to the layer method of [3] which produces spurious noise. Further improvement may be obtained by either a pre- or postprocessing of the images or by using optimal estimation techniques.

#### References

- [1] Roerdink, J. B. T. M., "FFT-based methods for nonlinear image restoration in confocal microscopy," *J. Math. Imaging and Vision*, 4, no. 2, pp. 199–207, 1996, pp. 55-63.
- [2] Roerdink, J. B. T. M. and Bakker, M., "An FFT-based method for attenuation correction in fluorescence confocal microscopy," *J. Microscopy*, 169, pp. 3–14, 1993.
- [3] Visser, T. D., Groen, F. C. A. and Brakenhoff, G. J., "Absorption and scattering correction in fluorescence confocal microscopy," *J. of Microscopy*, 163, pp. 189–200, 1991.

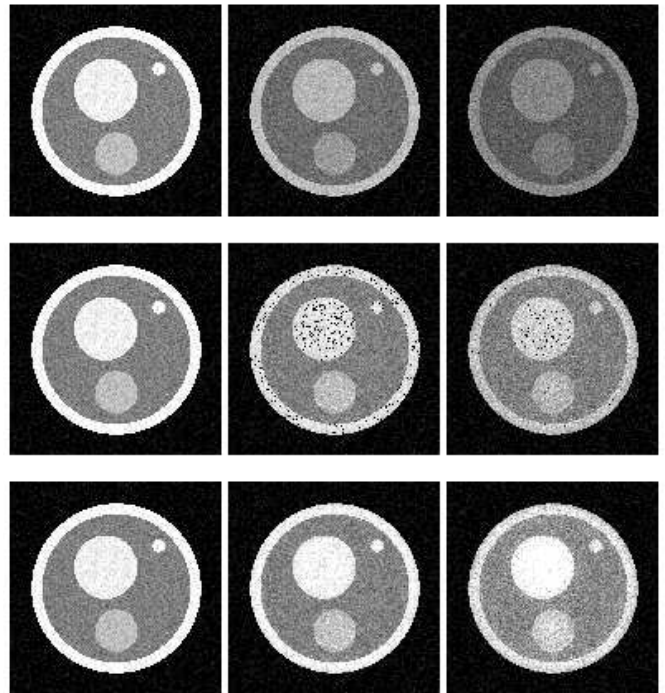


Figure 3: *Restoration of the circle image perturbed by Gaussian noise (see text).*

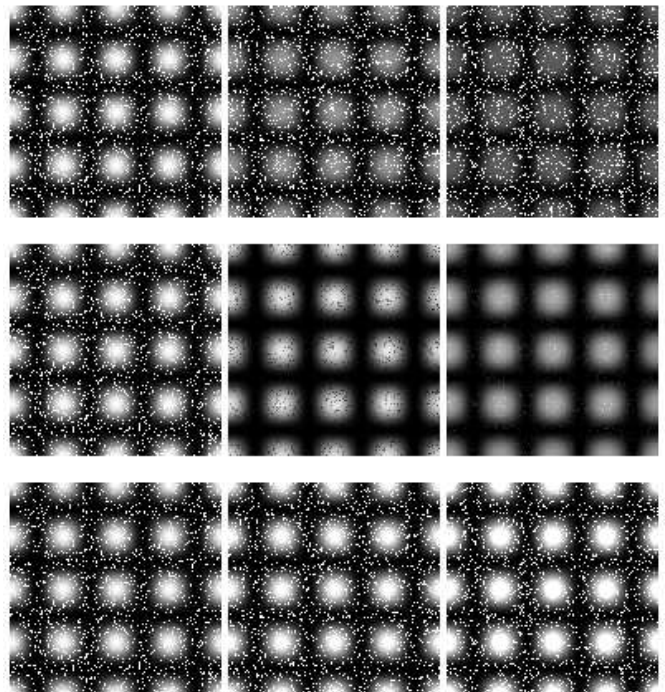


Figure 4: *Restoration of the trig image perturbed by Poisson noise (see text).*